Site-Specific Glycosylation of Human Recombinant Erythropoietin: Analysis of Glycopeptides or Peptides at Each Glycosylation Site by Fast Atom Bombardment Mass Spectrometry†

Hiroshi Sasaki,‡,§ Norimichi Ochi,∥ Anne Dell,⊥ and Minoru Fukuda*,‡

La Jolla Cancer Research Foundation, Cancer Research Center, La Jolla, California 92037, Fuji-Gotemba Research Laboratories, Chugai Pharmaceuticals Company, Ltd., Shizuoka, Japan, and Department of Biochemistry, Imperial College of Science and Technology, London, Great Britain

Received March 10, 1988; Revised Manuscript Received May 31, 1988

ABSTRACT: We have previously determined the carbohydrate structure of human recombinant erythropoietin [Sasaki, H., Bothner, B., Dell, A., & Fukuda, M. (1987) *J. Biol. Chem. 262*, 12059–12076]. The carbohydrate chains are distributed in three N-glycosylation sites and one O-glycosylation site. In order to examine the extent to which protein structure influences glycosylation, we have analyzed the saccharide structures at each glycosylation site (Asn^{24}, Asn^{38}, Asn^{83}, and Ser^{126}) of human recombinant erythropoietin. By high-performance liquid chromatography, we have succeeded in separation of glycopeptides containing different O-linked saccharides to the same peptide backbone. Fast atom bombardment mass spectrometry of the isolated glycopeptides combined with Edman degradation allowed us to elucidate the composition of glycopeptides and the amino acid attachment site. The analysis of glycopeptides and saccharides by fast atom bombardment mass spectrometry and high-performance liquid chromatography provided the following conclusions on *N*-glycans: (1) saccharides at Asn^{24} are heterogeneous and consist of biantennary, triantennary, and tetraantennary saccharides with or without *N*-acetyllactosaminyl repeats; (2) saccharides at Asn^{38} mainly consist of well-processed saccharides such as tetraantennary saccharides with or without *N*-acetyllactosaminyl repeats; (3) saccharides at Asn^{83}, on the other hand, are homogeneous in the backbone structure and are composed mainly of tetraantennary without *N*-acetyllactosaminyl repeats. It was also noted that saccharides at Asn^{24} are much less sialylated than those at Asn^{38}, although these two glycosylation sites are close to each other. These results clearly indicate that the protein structure and, possibly, the carbohydrate chain at the neighboring site greatly influence glycosylation of a given glycosylation site.

Erythropoietin is a glycoprotein hormone which stimulates proliferation and differentiation of erythroid precursor cells to mature erythrocytes (Goldwasser et al., 1968; Miyake et al., 1977). Although purified erythropoietin is essential for understanding molecular mechanisms of erythropoiesis and treatment of anemia, it has been extremely difficult to obtain the erythropoietin in quantity from natural sources. In order to overcome this problem, cDNA clones for human erythropoietin have been isolated (Jacobs et al., 1985; Lin et al., 1985; Powell et al., 1986), and the recombinant erythropoietin produced in mammalian cells has been successfully used to reverse the anemia of patients with renal disease (Winearles et al., 1986; Eschbach et al., 1987). Similar treatments have been suggested also for anemic patients with rheumatoid arthritis (Baer et al., 1987) and sickle cell disease (Al-Khatti et al., 1987).

It has been noted that the carbohydrate moiety of erythropoietin is essential for its function in vivo (Rambach et al., 1958; Lowy et al., 1960; Lukowsky et al., 1972; Goldwasser et al., 1974). We have recently analyzed the carbohydrate structure of human erythropoietin produced by transfection of Chinese hamster ovary cells with cDNA (Sasaki et al., 1987). Our studies showed that erythropoietin contains mainly tri- or tetraantennary saccharides with or without one or two *N*-acetyllactosaminyl repeats. Further, we have also elucidated the structures of O-linked saccharides (Sasaki et al., 1987). Since N-linked saccharides attach to three glycosylation sites and O-linked saccharides to one site (Lai et al., 1985; Recny et al., 1987), this glycoprotein serves as a good model for the analysis of carbohydrate moieties. In this paper, we have asked the following questions: (1) How heterogeneous are carbohydrate chains at each site? (2) What are the differences between the N-linked carbohydrate chains among the three attachment sites? These studies were carried out by fractionating glycopeptides and analyzing the carbohydrate or peptide moiety attached to each glycosylation site by fast atom bombardment mass spectrometry.

Experimental Procedures

Erythropoietin. Erythropoietin was purified from the spent medium of Chinese hamster ovary cells, which were transfected with an expression vector containing the human erythropoietin cDNA (Jacobs et al., 1985). The purification procedure was modified from that of Miyake et al. (1977) and essentially followed the procedure of Jacobs et al. (1985).

Proteolytic Digestion of Erythropoietin and Fractionation of Peptides by High-Performance Liquid Chromatography.

† This work was supported by Grant R01 CA33000 from the National Cancer Institute and by a program grant from the British Medical Research Council.

* To whom correspondence should be addressed at the La Jolla Cancer Research Foundation, 10901 N. Torrey Pines Rd., La Jolla, CA 92037.

‡ La Jolla Cancer Research Foundation.

§ On leave from Fuji-Gotemba Research Laboratories, Chugai Pharmaceuticals Co., Ltd., Shizuoka, Japan.

∥ Chugai Pharmaceuticals Co., Ltd.

⊥ Imperial College of Science and Technology.

0006-2960/88/0427-8618$01.50/0

Erythropoietin (1 mg of protein) was reduced with 2-mercaptoethanol and pyridylethylated according to the procedure described (Recny et al., 1987). The pyridylethylated sample was then adjusted to pH 2.0 by 10% trifluoroacetic acid in water and purified by high-performance liquid chromatography (HPLC)[1] as described below. Pyridylethylated erythropoietin was recovered by lyophilization and digested with endoproteinase Lys-C (Boehringer Manheim), which cleaves peptide bonds at the carboxyl side of lysine residues (Jakel et al., 1983). The resultant peptides were then fractionated by reverse-phase HPLC using a column (4.6 × 250 mm) of Bio-Rad RP-318 (C18). The column was initially equilibrated with solvents A, 0.1% trifluoroacetic acid, and B, 90% acetonitrile in 0.1% trifluoroacetic acid (90:10). The column was eluted in four steps in which the concentration of solvent B was gradually increased (see Figure 1A). The flow rate was 1 mL/min.

Separation of Glycopeptides Containing O-Linked Oligosaccharides. In order to further separate glycopeptides containing O-linked saccharides, one of the fractions obtained above (K6) was digested by trypsin and fractionated by HPLC using a column of μBondapak C-18 (Waters). The column was equilibrated with 20 mM NH_4HCO_3, pH 7.4. After the column was washed with the same solution for 5 min, the column was eluted with a linear gradient from the same buffer to acetonitrile/20 mM NH_4HCO_3, pH 7.4 (60:40), over 60 min. The flow rate was 1 mL/min, and each 0.5 mL/fraction was collected.

Isolation of N-Linked Saccharides from Glycopeptides. The glycopeptides were digested with *Flavobacterium meningosepticum N*-glycanase (Plummer et al., 1984) (Genzyme). The digests were reduced with NaB^3H_4 and fractionated by Sephadex G-50 gel filtration as described previously (Sasaki et al., 1987).

Fractionation of Saccharides by HPLC. Intact oligosaccharides were fractionated by anion-exchange HPLC employing a Toyosoda TSK-DEAE 2SW column. Neutral oligosaccharides, obtained after desialylation by mild acid hydrolysis, were separated by HPLC with a column (0.4 × 25 cm) of Lichrosorb-NH_2 (5-μm particle size, Merck). These chromatographic procedures were described earlier in detail (Sasaki et al., 1987). HPLC was carried out with a Varian HPLC apparatus (Model 5000, Varian Associates, Inc.).

Fast Atom Bombardment Mass Spectrometry. FAB-MS of intact glycopeptides and peptides was carried out essentially in the same way as described (Robb et al., 1984; Fukuda et al., 1986). Oligosaccharides were released from O-linked glycopeptides and permethylated in a single-step reaction using the procedure which Ciucanu and Kerek (1984) showed to be suitable for permethylating oligosaccharides. The glycopeptide was dissolved in dimethyl sulfoxide (100 μL), and dry, powdered NaOH (0.5 mg) was added followed by methyl iodide (0.5 mL). The resulting mixture was shaken for 10 min at room temperature, quenched with water, and extracted into chloroform. The chloroform layer was washed 5 times with 2 mL of water and dried under a stream of nitrogen, and the products were analyzed by FAB-MS without further purification. Esterification of the carboxyl groups of the methylated sample was made by dissolving the sample in methanol (100 μL) and adding 500 μL of an ether solution of dry distilled diazomethane. The reaction was left at room temperature for 40 min, and the reagents were removed under nitrogen. Products were analyzed by FAB-MS without further purification.

[1] Abbreviations: HPLC, high-performance liquid chromatography; Endo Lys-C, endoproteinase Lys-C; FAB-MS, fast atom bombardment mass spectrometry; EtPy, pyridylethyl group; Lac, *N*-acetyllactosaminyl repeat.

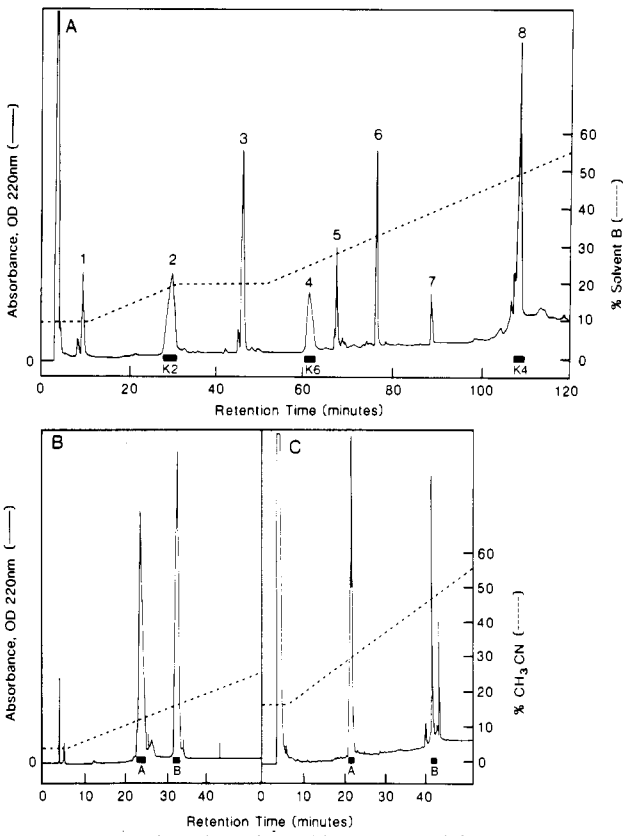

FIGURE 1: Fractionation of peptides generated from recombinant human erythropoietin. (A) The pyridylethylated erythropoietin was digested with Endo Lys-C and subjected to reverse-phase HPLC using a column of Bio-Rad RP-318. The column was equilibrated with 0.1% trifluoroacetic acid/H_2O and 90% acetonitrile in 0.1% trifluoroacetic acid/H_2O (90:10). The elution was carried out by increasing the concentration of the 90% acetonitrile in 0.1% trifluoroacetic acid (solution B), which is indicated by the dashed line. (B) Peak 2 (peptide K2) in (A) was digested with V8 protease and subjected to the same HPLC, except for a difference in the elution condition. (C) Peak 8 (peptide K4) in (A) was digested with trypsin and subjected to the same HPLC, except for the difference in the elution condition. In (B) and (C), the elution was carried out by increasing the concentration of acetonitrile in 0.1% trifluoroacetic acid/H_2O, which is indicated by dashed lines.

Amino Acid Sequence Analysis. Peptides were subjected to Edman degradation using a gas-phase protein sequencer, 470A (Applied Biosystems). The resultant phenylthiohydantoin (PTH) derivatives were analyzed in a PTH analyzer, 120A (Applied Biosystems) (Grant et al., 1983).

RESULTS

Fractionation of Peptides and Glycopeptides. Peptides and glycopeptides obtained by Endo Lys-C digestion of recombinant erythropoietin were fractionated by reverse-phase HPLC, as shown in Figure 1A. Amino acid sequence analysis of each peak indicates that these peaks correspond to the following peptide fragments; 1, K9; 2, K2; 3, K3; 4, K6; 5, K7; 6, K1; 7, K5; 8, K4. The peptides K1–K9 are derived from the erythropoietin molecule as shown in Figure 2 (Lai et al., 1986; Recney et al., 1987). From the amino acid sequence analysis, it was determined that K6 contains O-linked saccharides whereas K2 and K4 contain N-linked saccharides.

Fractionation of Glycopeptides Containing O-Linked Saccharides. K6 peptide was trypsinized to yield a glycopeptide which presumably contains residues 117–131 (see Figure 3).

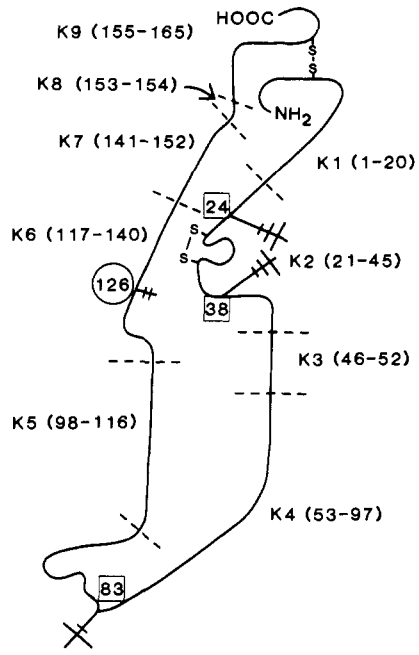

FIGURE 2: Predicted structure of human erythropoietin [adopted from references of McDonald et al. (1986) and Recny et al. (1987)]. K1–K9 are peptides generated by Endo Lys-C, and the amino acid residue numbers are indicated in parentheses. The amino acid residues 24, 38, and 83 attach N-linked saccharides, whereas residue 126 attaches O-linked saccharides.

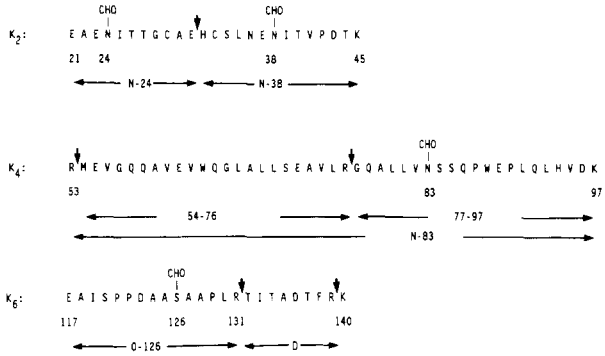

FIGURE 3: Amino acid sequence of glycopeptides obtained from human recombinant erythropoietin. Glycopeptides were obtained by Endo Lys-C digestion of pyridylethylated erythropoietin. CHO indicates the carbohydrate moiety. K2: The arrow indicates the position where V8 protease presumably cleaves the peptide bond. K4 and K6: The arrows indicate the positions where trypsin presumably cleaves the peptide bonds. After *N*-glycanase digestion, asparagine (N) at residues 24, 38, and 83 was converted to aspartic acid (D).

The trypsinized sample was then subjected to HPLC using a μBondapack C-18 column, as shown in Figure 4. The glycopeptides were resolved into four fractions, and each fraction was subjected to FAB-MS analysis.

Structural Characterization of Fraction A. FAB-MS of intact fraction A provided a major ion at m/z 2412 corresponding to the molecular ion for $NeuNAc_2$·Hex·HexNAc linked to the peptide EAISPPDAASAAPLR (Figure 5A). Additional signals were present at m/z 2121 and 1830, which correspond in composition to NeuNAc·Hex·HexNAc and Hex·HexNAc, respectively, linked to the same peptide. Either these ions could be molecular ions of glycopeptides with truncated sugar chains or they could be formed in the ion source by β cleavages of the ion at m/z 2412 [see Dell (1987) for details]. These possibilities can be readily distinguished by releasing the oligosaccharide(s) from the peptide and subjecting the permethylated derivative to FAB-MS. We have

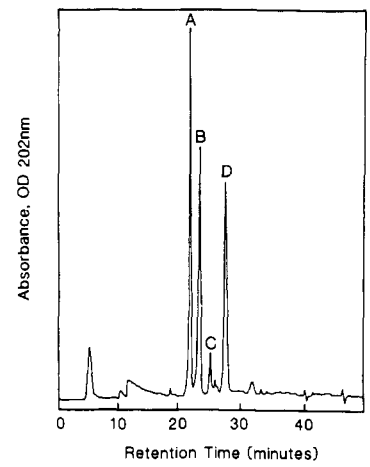

FIGURE 4: Separation of glycopeptides containing O-linked saccharides by reverse-phase HPLC. K6 peptide (peak 4 in Figure 1A) was digested by trypsin and applied to a column of μBondapack C-18 equilibrated with 20 mM NH_4HCO_3, pH 7.4. After being washed with the same buffer for 5 min, the column was eluted with a linear gradient from the same buffer to 60% acetonitrile in 20 mM NH_4HCO_3, pH 7.4, over 55 min. *Ordinate*, relative intensity at 202 nm; *abscissa*, retention time in minutes.

found the NaOH/methyl iodide permethylation procedure of Ciucanu and Kerek (1984) to be a convenient and novel one-step method for an effective release and methylation of O-linked carbohydrates. The products of NaOH/methyl iodide treatment of fraction A afforded the spectrum shown in Figure 5B. The major molecular ion at m/z 1190 corresponds to doubly undermethylated $NeuNAc_2$·Hex·HexNAc. Fragment ions at m/z 330 (m/z 362 minus methanol) and m/z 362 (undermethylated $NeuNAc^+$) indicated that the undermethylation is, in fact, lack of esterification of the sialic acid residues. This was confirmed by diazomethane esterification which shifted m/z 1190 to m/z 1218, the mass expected for the fully methylated tetrasaccharide. Importantly, there are no signals which correspond to the molecular ions of shorter oligosaccharides (Figure 5C). Therefore, the signals at m/z 2121 and 1830 in Figure 5A are, indeed, fragment ions, and peak A contains the single glycopeptide $NeuNAc_2$·Hex·HexNAc attached to EAISPPDAASAAPLR.

This peptide contains two potential glycosylation sites at positions 4 and 10 (Figure 3). To define the carbohydrate attachment site, we subjected the glycopeptide to Edman degradation followed by FAB-MS to define the mass of the truncated peptide and glycopeptide. The first potential glycosylation site is removed after four steps of the Edman reaction. The products obtained after the fourth cycle gave the FAB spectrum shown in Figure 5D. The signals at m/z 1430, 1452, and 1468 correspond to $[M + H]^+$, $[M + Na]^+$, and $[M + K]^+$ for the glycopeptide containing Hex·HexNAc attached to PPDAASAAPLR. The sialic acid residues were lost during the acid-catalyzed cyclization step of the Edman degradation. These assignments were corroborated by subjecting the remainder of the sample to a fifth cycle of the Edman degradation. This treatment afforded a new signal at m/z 1333 which is one proline less than m/z 1430 (Figure 5E). The results confirmed that the K6 peptide is glycosylated at position 10 (residue 126) (see Figure 3).

Structural Characterization of Fraction B. FAB-MS of fraction B (Figure 6A) provided a prominent signal at m/z 2121 corresponding to the molecular ion for NeuNAc·Hex·HexNAc attached to the peptide EAISPPDAASAAPLR. This ion was associated with the fragment ions corresponding to Hex·HexNAc attached to the peptide (m/z 1830), HexNAc

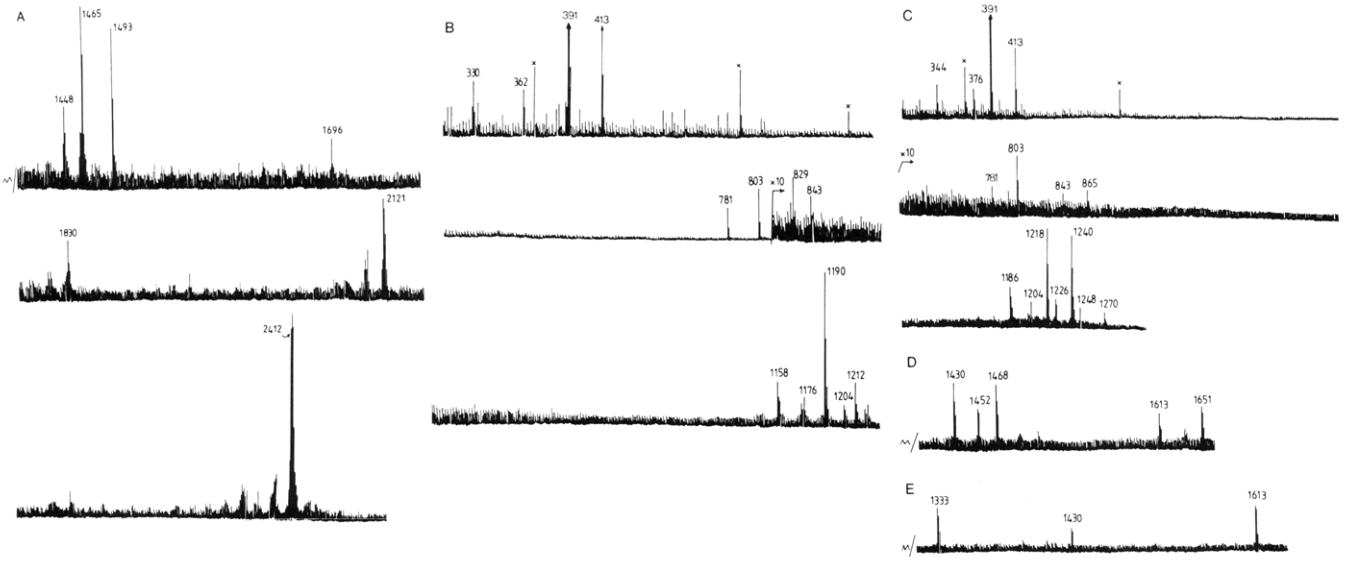

FIGURE 5: Fast atom bombardment mass spectra of the glycopeptide containing disialosyl O-linked saccharide (peak A in Figure 4). The positive spectra were recorded. (A) Intact glycopeptide A. The major signal at m/z 2412 corresponds to $NeuNAc_2$·Hex·HexNAc attached to the peptide EAISPPDAASAAPLR. The ions at m/z 2121, 1830, and 1465 correspond to the molecular ions minus NeuNAc, $NeuNAc_2$, and $NeuNAc_2$·Hex·HexNAc. Under these conditions, these ions either could be derived by β cleavage of the parent molecule or could represent molecular ions which lack those glycosyl residues. The signals at m/z 1493 and 1696 are the result of ring cleavages. (B) Glycopeptide A in Figure 4 after methylation. Glycopeptide A was methylated with NaOH and methyl iodide and subjected to analysis. Signals at m/z 1158, 1190, and 1212 correspond to A-type, $[M + H]^+$, and $[M + Na]^+$ molecular ions for di-undermethylated $NeuNAc_2$·Hex·HexNAc. Signals at m/z 330 (362 − methanol) and 362 (undermethylated $NeuNAc^+$) locate the undermethylation on the sialic acids. Signals at m/z 829 and 843 are β-cleavage ions. Signals at m/z 391, 413, 781, and 803 correspond to $[M + H]^+$, $[M + Na]^+$, $[2M + H]^+$, and $[2M + Na]^+$ ions for a contaminant, dioctyl phthalate. (C) FAB-MS of the sample which gave spectrum B after esterification with diazomethane. The major signals at m/z 1186, 1218, and 1240 correspond to A-type, $[M + H]^+$, and $[M + Na]^+$ molecular ions for fully methylated $NeuNAc_2$·Hex·HexNAc. Minor signals at m/z 1204, 1226, 1248, and 1270 correspond to $[M + H]^+$ and Na adducts of undermethylated material. Signals at m/z 843 and 865 (Na adducts of 843) are β-cleavage ions; m/z 344 and 376 are due to $NeuNAc^+$. The contaminant (m/z 319, 413, 781, and 803) observed in (B) is also present. (D) Glycopeptide A after four cycles of Edman degradation. The ions at m/z 1430, 1452, and 1468 correspond to $[M + H]^+$, $[M + Na]^+$, and $[M + K]^+$ for Hex·HexNAc attached to PPDAASAAPLR. The ions at m/z 1613 and 1651 correspond to $[M + H]^+$ and $[M + K]^+$ for Hex·HexNAc attached to the trifluoroacetylated derivative of SPPDAASAAPLR. The sialic acids were hydrolyzed during the trifluoroacetic acid cleavage steps of the Edman degradation, and the trifluoroacetylated byproduct was also formed during the reaction. (E) Glycopeptide A after five cycles of Edman degradation. In order to obtain better data on a small amount of the sample available for this experiment, acid dosing was used. The majority of the signal at m/z 1430 (Figure 5D) shifted to m/z 1333, indicating the removal of proline from PPDAASAAPLR. However, the signal at m/z 1613 remained, since a trifluoroacetylated NH_2 terminal prevents further derivatization for Edman degradation. This experiment, therefore, confirmed the assignment of m/z 1430 and 1613.

attached to the peptide (m/z 1696), and the peptide (m/z 1465).

These latter ions were produced by β cleavage of the parent molecule since FAB-MS of the permethylated sample yielded molecular ions for NeuNAc·Hex·HexNAc only (Figure 6B). These results indicate that fraction B is NeuNAc·Hex·HexNAc attached to the peptide EAISPPDAASAAPLR.

Fraction C and Fraction D. FAB-MS of fraction C and fraction D indicates that fraction C is Hex·HexNAc attached to the peptide EAISPPDAASAAPLR (Figure 6C) and fraction D is the peptide TITADTFR (Figure 7A). The latter peptide was produced from the carboxy-terminal half of K6 peptide by tryptic digestion (see Figure 3).

Isolation of N-Linked Saccharides from Glycopeptides. Since peptide K2 contains two N-linked saccharides (see Figure 3), the peptide was digested by V8 protease and subjected to HPLC. Figure 1B shows that resultant peptides were resolved into two products, and it was found by amino acid sequence analysis that fraction A corresponds to the peptide containing Asn^{24} and fraction B corresponds to the peptide containing Asn^{38}. Hereafter, the N-linked glycopeptides are called N-24, N-38, and N-83, based on the residue number of the asparagine to which saccharides are linked.

Each glycopeptide was digested by *N*-glycanase, and the digests were reduced by NaB^3H_4. The samples were then applied to a column of Sephadex G-50 to separate saccharides from peptides as shown in Figure 8. Saccharides and peptides obtained from N-24 and N-38 were separated whereas those from N-83 could not be resolved.

In order to confirm the identity of N-24 and N-38, which were derived from the peptide K2, peptides released from N-24 and N-38 glycopeptides (Figure 8A,B) were subjected to FAB-MS. The results shown in Figure 7 confirmed that N-24 and N-38 correspond to the respective glycopeptides containing residues 21–31 and residues 32–45. During the analysis of peptide N-38, we also detected other ions which correspond to truncated peptides originally present in the sample (Figure 7C). These results confirmed not only the composition of N-38 but also the amino acid sequence of N-38.

To confirm the third N-glycosylation site, K4 peptide was digested with trypsin and subjected to HPLC (Figure 1C). Sequence analysis of fraction A in Figure 1C provided the sequence identical with residues 77–97 except that residue 83 was aspartic acid, which was converted from asparagine after *N*-glycanase treatment (Plummer et al., 1984).

Analysis of N-Linked Saccharides Attached to N-24, N-38, and N-83 Glycopeptides after Desialylation. A portion of the saccharides after Sephadex G-50 gel filtration (Figure 8) was desialylated and subjected to HPLC with a Lichrosorb column. As described previously under these conditions, the saccharides can be separated according to the number of *N*-acetyllactosaminyl units (Sasaki et al., 1987). As shown in Figure 9A, saccharides from N-24 contain all of the molecular species originally present in the whole molecule. However, the amount

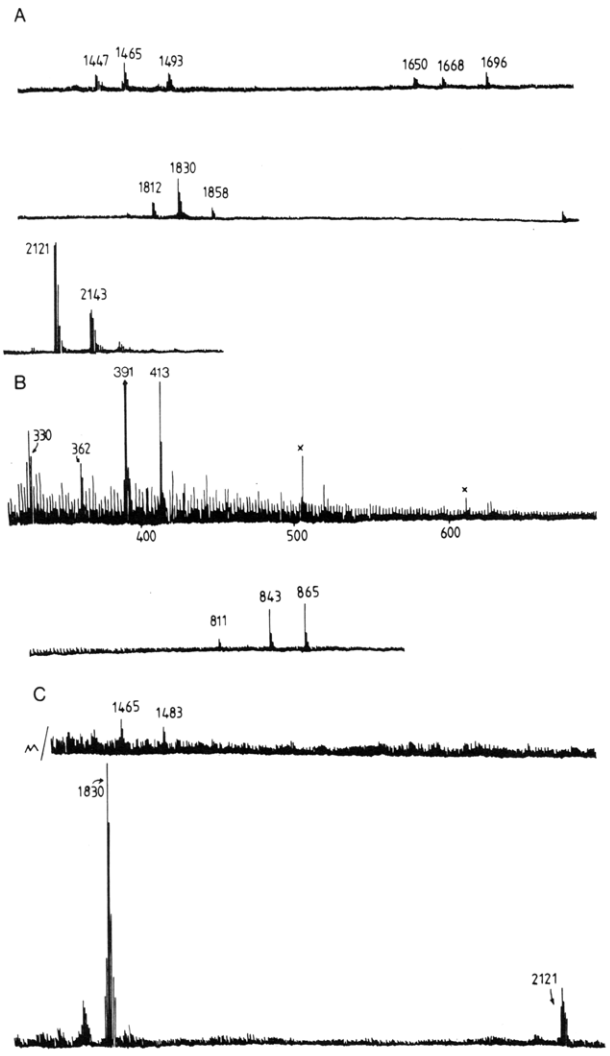

FIGURE 6: FAB-MS of glycopeptide B and glycopeptide C. The positive spectra were obtained. (A) Glycopeptide B in Figure 4 before methylation. The prominent ions at m/z 2121 and 2143 correspond to $[M + H]^+$ and $[M + Na]^+$ for NeuNAc·Hex·HexNAc attached to the peptide EAISPPDASAAPLR. The ions at m/z 1830, 1696, and 1465 correspond to the ions lacking NeuNAc, NeuNAc·Hex, and NeuNAc·Hex·HexNAc, respectively, from the parent molecule. These ions were determined to be the products of β cleavage based upon FAB-MS of the permethylated sample [see (B)]. Signals 18 mass units below each of the above ions are derived from loss of water; signals 28 mass units higher are the result of a ring cleavage reaction as described (Dell, 1987). (B) Glycopeptide B after methylation. Glycopeptide B was treated with NaOH and methyl iodide and analyzed without esterification. The signals at m/z 811, 843, and 865 correspond to the A-type ion, $[M + H]^+$, and $[M + Na]^+$, respectively, of permethylated NeuNAc·Hex·HexNAc lacking one methyl group. Signals at m/z 330 (362 minus methanol) and 362 (undermethylated $NeuNAc^+$) define the site of undermethylation. No signals are present for the Hex·HexNAc molecular ion. Signals at m/z 391 and 413 are explained in the legend to Figure 5B. (C) Intact glycopeptide C in Figure 4. The prominent ion m/z 1830 corresponds to the molecular ion for Hex·HexNAc attached to the peptide EAISPPDASAAPLR. This sample also contained a small amount of NeuNAc·Hex·HexNAc attached to the same peptide since a weak signal was detected at m/z 2121. However, the signal at m/z 1830 is much more prominent than that of m/z 2121, indicating that the majority of the m/z 1830 signal was not derived by β cleavage of the ion at m/z 2121 (see also Figures 5A and 6A). Signals at m/z 1465 and 1493 are defined in the legend to Figure 5A.

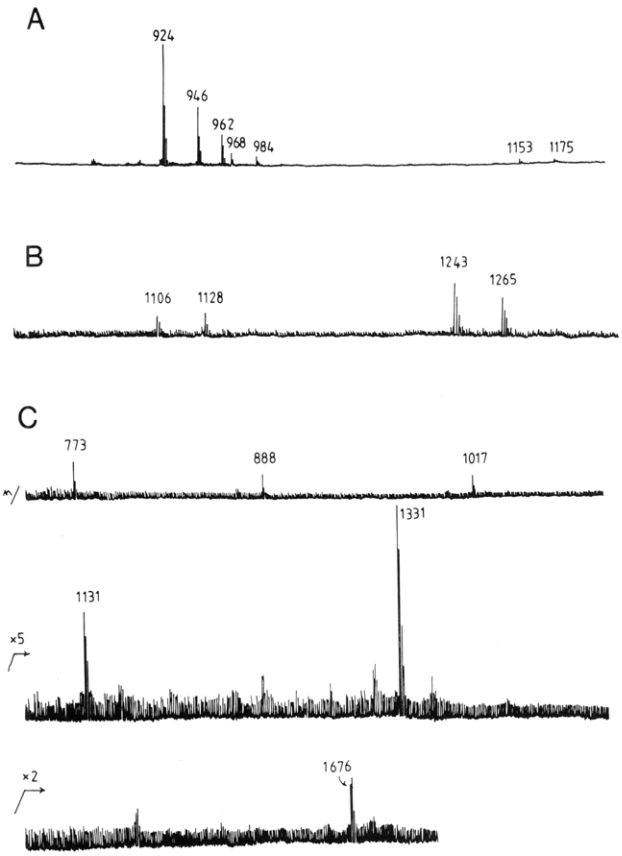

FIGURE 7: Fast atom bombardment mass spectra of peptides obtained from 0–126 (K6), N-24, and N-38 glycopeptides. The positive spectra were obtained on carbohydrate-free peptides. (A) Fractions 54–56, peptide D in Figure 4 (tryptic peptide from K6). The prominent ions at m/z 924, 946, and 962 correspond to $[M + H]^+$, $[M + Na]^+$, and $[M + K]^+$ for TITADTFR. Minor signals at m/z 1153 and 1175 could correspond to residues 41–50 or 135–143. (B) Fractions 47–52 in Figure 8A (N-24). The prominent ions at m/z 1243 and 1265 correspond to the molecular ion and its Na adduct for EAEDITTG-(EtPy–)CAE. The ions at m/z 1106 and 1128 are probably due to a contaminating peptide of m/z 1106 which could be residues 18–27. (C) Fractions 55–65 in Figure 8B (N-38). The prominent ion at m/z 1676 corresponds to the molecular ion for H(EtPy–)CSLNED-ITVPDTK. The other significant ions at m/z 773, 888, 1017, 1131, and 1331 correspond to ITVPDTK, DITVPDTK, EDITVPDTK, NEDITVPDTK, and SLNEDITVPDTK, respectively.

of biantennary and triantennary saccharides was noticeably higher than in the saccharides from the whole molecule (Table I). The saccharides from N-83 glycopeptide, on the contrary, contain almost exclusively tetraantennary form together with a small amount of triantennary and tetraantennary forms with one *N*-acetyllactosaminyl repeat (Figure 9C and Table I). Saccharides from N-38, on the other hand, consist of triantennary, tetraantennary, and tetraantennary forms with one or two *N*-acetyllactosaminyl repeats (Figure 9B and Table I). These results clearly indicate that Asn^{24}, Asn^{38}, and Asn^{83} attach quite different sets of saccharides and molecular species attached to Asn^{24} or Asn^{38} are more heterogeneous than those attached to Asn^{83}.

Analysis of Sialylated N-Linked Saccharides Attached to Asn^{24}, Asn^{38}, and Asn^{83}. Figure 10 shows that the ratio of monosialosyl, disialosyl, and trisialosyl forms differs considerably among saccharides attached to Asn^{24}, Asn^{38}, and Asn^{83}. Further, the amount of each peak in disialosyl and trisialosyl saccharides reflects the molecular species present in different attachment sites. For example, III-1 and III-2, which contain trisialyl forms with two and one *N*-acetyllactosaminyl repeat, are much more prominent in N-24 or N-38 saccharides than N-83 saccharides. Similarly, II-1 and II-2 are almost absent in N-83 saccharides, being consistent with the absence of molecules with *N*-acetyllactosaminyl repeats. In another aspect, N-24 saccharides are sialylated to a much lesser extent

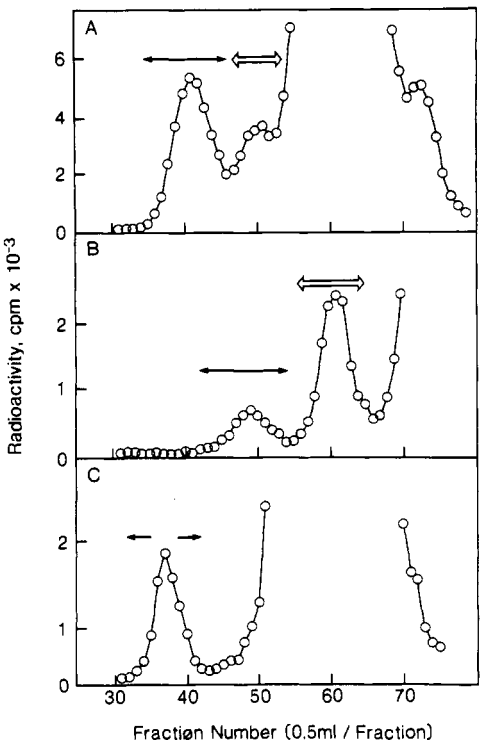

FIGURE 8: Sephadex G-50 gel filtration of *N*-glycanase digests of N-24, N-38, and N-83 glycopeptides. The digests, after reduction with NaB^3H_4, were subjected to Sephadex G-50 gel filtration under similar conditions as described previously (Sasaki et al., 1987). From N-24 (A) and N-38 (B) glycopeptides, saccharides (indicated by closed horizontal arrows) and peptides (indicated by open horizontal arrows) were obtained. From N-83 glycopeptides (C), saccharides and the peptide were recovered in the same fraction (indicated by horizontal arrows). Each fraction contained 0.5 mL. The size of columns was 1.0 × 32 cm for (A) and (C) and 1.0 × 35 cm for (B).

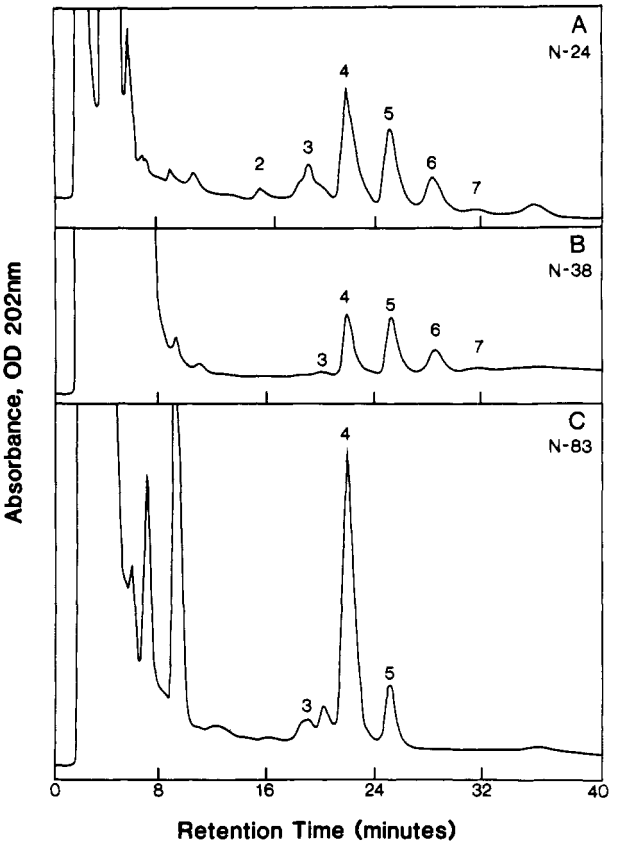

FIGURE 9: HPLC of asialo N-linked saccharides derived from N-24, N-38, and N-83 glycopeptides. N-Linked saccharides were desialylated by mild acid hydrolysis and applied to a 5-μm Lichrosorb-NH_2 column under the same conditions as described (Sasaki et al., 1987). Briefly, the column was equilibrated with acetonitrile/10 mM potassium phosphate buffer, pH 4.5 (65:35). The column was then eluted with a linear gradient to acetonitrile/10 mM potassium buffer, pH 4.5 (39:61), over 60 min. The fractions were indicated by the same numbers as described previously (Sasaki et al., 1987).

than N-38 saccharides, although they contain a very similar set of saccharides after desialylation. Only a part of monosialosyl forms in N-24 saccharides were accounted by the presence of biantennary forms, which were found to contain exclusively one sialic acid (Sasaki et al., 1987). These results indicate that saccharides at each glycosylation site differ considerably from those at another site.

Discussion

The present study demonstrates the usefulness of FAB-MS for analysis of glycopeptides, particularly those containing O-linked saccharides. First, FAB-MS is an excellent technique for defining the molecular weights of O-linked glycopeptides at the microgram level. Provided the peptide sequence and the nominal mass of the total amino acid content are known, the carbohydrate compositions are defined by the molecular weights. This is an extension of the results obtained by Townsend et al. (1984), who showed the usefulness of FAB-MS analysis of *N*-glycan-containing peptides. Second, FAB-MS of permethylated samples provides information on saccharide sequences and heterogeneity as well as confirming the interpretation of fragment ions obtained on intact molecules. We also noticed that the methylation method of Ciucanu and Kerek was not powerful enough for esterification of carboxyl groups of sialic acid residues (Figure 5B). Since we have never experienced underesterification of sialic acid by Hakomori's method (Hakomori, 1964), these two methods differ in this aspect. Third, it is possible to identify the amino acid residue to which is attached the carbohydrate by Edman degradation followed by FAB-MS. On the basis of the nominal mass of the total amino acid content and peptide sequence determined previously, this procedure allows us to obtain the amino acid sequence on a sample with less than 1 nmol. This method is feasible without a more expensive instrument such as tandem mass spectrometry (Johnson & Biemann, 1987). However, the latter method does not require prior knowledge of the peptide sequence. FAB-MS is useful for identifying the amino acid residues to which N-linked saccharides are attached in glycoproteins of known peptide sequence since FAB-MS will reveal the presence of Asp rather than Asn in peptide products of *N*-glycanase digestion, as shown previously (Carr & Roberts, 1986). It is also possible to obtain the molecular weights of *N*-glycans released from glycopeptides when they are of relatively small molecular weights. However, the amount required for the analysis of oligosaccharides is much higher than for peptides and glycopeptides. This is also true for the analysis of oligosaccharides by cesium ion liquid secondary ion mass spectrometry (Gillece-Castro et al., 1987).

The present study also established a method for isolation of glycopeptides and analysis of their carbohydrate moieties. We found, unexpectedly, that the behavior of glycopeptides during reverse-phase HPLC is heavily dependent on the property of its peptide under selected conditions. For example, Asn^{24} glycopeptide eluted earlier from the column than K2 glycopeptide which consists of Asn^{24} and Asn^{38} glycopeptides (see Figure 3). This behavior can be partly predicted from the hydrophobicity of its peptide calculated as described (Meek, 1980). Thus, it is possible to isolate glycopeptides at

Table I: Structures of Asialo N-Linked Saccharides Obtained from Human Recombinant Erythropoietin[d]

structure[a]	N-24, N-38, N-83
Bi-antennary	
Galβ1→4GlcNAcβ1→2Manα1 (6) Fuc α1 (6) Manβ1→4GlcNAcβ1→4GlcNAcOH; Galβ1→4GlcNAcβ1→2Manα1 (3)	6% 0 0
Tri-antennary	
Galβ1→4GlcNAcβ1→2Manα1 (6) Fuc α1 (6) Manβ1→4GlcNAcβ1→4GlcNAcOH; Galβ1→4GlcNAcβ1→4 (Manα1→3) Galβ1→4GlcNAcβ1→2Manα1 (3)	15% 5% 6%
Galβ1→4GlcNAcβ1→6 (Manα1→2 Galβ1→4GlcNAcβ1) Fuc α1 (6) Manβ1→4GlcNAcβ1→4GlcNAcOH; Galβ1→4GlcNAcβ1→2Manα1 (3)	
Tetra-antennary[b]	
Galβ1→4GlcNAcβ1→6 (Manα1→2 Galβ1→4GlcNAcβ1) Fuc α1 (6) Manβ1→4GlcNAcβ1→4GlcNAcOH; Galβ1→4GlcNAcβ1→4 (Manα1→2) Galβ1→4GlcNAcβ1 (3)	45% 49% 85%
Tetra-antennary Lac$_1$	
Galβ1→4GlcNAcβ1→3Galβ1→4GlcNAcβ1→6 (Manα1→2 Galβ1→4GlcNAcβ1) Fuc α1 (6) Manβ1→4GlcNAcβ1→4GlcNAcOH; Galβ1→4GlcNAcβ1→4 (Manα1→2) Galβ1→4GlcNAcβ1 (3)	25% 32% 9%
Galβ1→4GlcNAcβ1→6 (Manα1→2 Galβ1→4GlcNAcβ1→Galβ1→4GlcNAcβ1) Fuc α1 (6) Manβ1→4GlcNAcβ1→4GlcNAcOH; Galβ1→4GlcNAcβ1→4 (Manα1→2) Galβ1→4GlcNAcβ1 (3)	
Galβ1→4GlcNAcβ1→6 (Manα1→2 Galβ1→4GlcNAcβ1) Fuc α1 (6) Manβ1→4GlcNAcβ1→4GlcNAcOH; Galβ1→4GlcNAcβ1→3Galβ1→4GlcNAcβ1→4 (Manα1→2) Galβ1→4GlcNAcβ1 (3)	
Tetra-antennary Lac$_2$	
Galβ1→4GlcNAcβ1→3Galβ1→4GlcNAcβ1→6 (Manα1→2 Galβ1→4GlcNAcβ1→3Galβ1→4GlcNAcβ1) Fuc α1 (6) Manβ1→4GlcNAcβ1→4GlcNAcOH; Galβ1→4GlcNAcβ1→4 (Manα1→2) Galβ1→4GlcNAcβ1 (3)	7% 10% 0
Galβ1→4GlcNAcβ1→3Galβ1→4GlcNAcβ1→6 (Manα1→2 Galβ1→4GlcNAcβ1) Fuc α1 (6) Manβ1→4GlcNAcβ1→4GlcNAcOH; Galβ1→4GlcNAcβ1→3Galβ1→4GlcNAcβ1→4 (Manα1→2) Galβ1→4GlcNAcβ1 (3)	
Tetra-antennary Lac$_3$[c]	
Galβ1→4GlcNAcβ1→3 Galβ1→4GlcNAcβ1→3 Galβ1→4GlcNAcβ1→3 (Galβ1→4GlcNAcβ1→6 (Manα1→2 Galβ1→4GlcNAcβ1) Fuc α1 (6) Manβ1→4GlcNAcβ1→4GlcNAcOH; Galβ1→4GlcNAcβ1→4 (Manα1→2) Galβ1→4GlcNAcβ1 (3))	2% 3% 0

[a] 15% of the saccharides lack fucose attached to reducing terminal *N*-acetylglucosamine. [b] A very small amount of triantennary Lac$_1$ is also present in this fraction. [c] A small portion of this saccharide contains (Galβ1 → 4GlcNAcβ1 → 3)$_3$ as a side chain. [d] The structures are based on previous work (Sasaki et al., 1987).

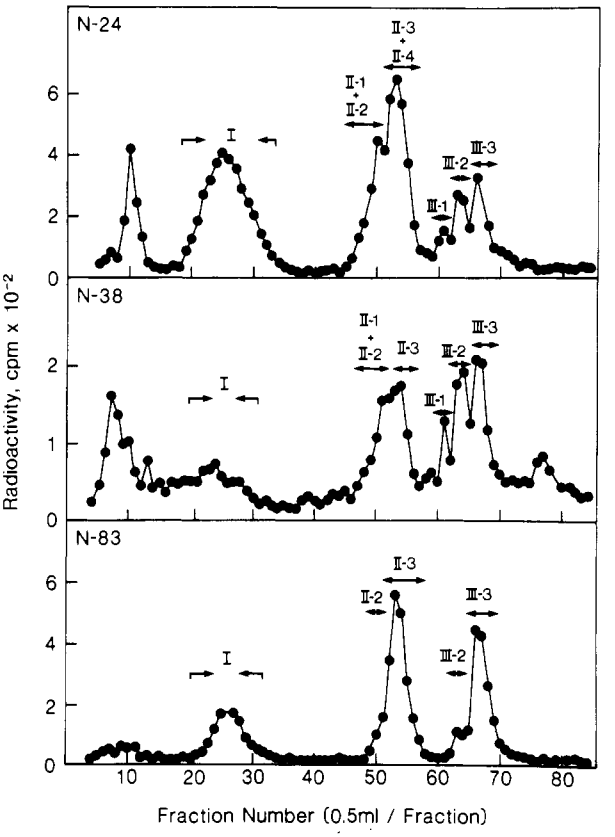

FIGURE 10: Ion-exchange HPLC of N-linked saccharides from N-24, N-38, and N-83 glycopeptides. N-linked saccharides obtained after Sephadex G-50 gel filtration (Figure 7) were applied to a column of TSK-DEAE 2SW equilibrated with 25 mM potassium phosphate buffer, pH 5.0. After being washed with the same buffer for 10 min, the column was eluted with a linear gradient from the same buffer to 400 mM potassium phosphate buffer, pH 5.0. The fractions were indicated by the same numbers as described previously (Sasaki et al., 1987). No carbohydrate was detected in other fractions. (Top) N-24 saccharides; (middle) N-38 saccharides; (bottom) N-83 saccharides.

each glycosylation in one fraction despite the fact that the carbohydrate moiety might be heterogeneous. As the second step, those isolated glycopeptides now can be separated according to the difference in the carbohydrate moiety, by increasing the pH of the column effluent. Alternatively, the carbohydrate moiety can be released from the glycopeptides by enzymatic or chemical treatment, and the released carbohydrate chains can be analyzed by HPLC on amino-bonded silica columns and/or by ion-exchange chromatography. During these analyses, we paid close attention to see if sialic acid is lost after various chromatographies. Judging from the ratio of sialylated saccharides shown in Figure 10, we saw no evidence of detectable loss of sialic acid. This conclusion is validated by the fact that N-24 and N-38 differ significantly in sialylation, despite the fact that both samples were produced by the same procedure.

The present study demonstrates the heterogeneity of carbohydrate chains among different N-glycosylation sites of human recombinant erythropoietin. The carbohydrate chains attached at Asn^{24} are composed of biantennary (6%), triantennary (15%), tetraantennary (45%), and tetraantennary with *N*-acetyllactosaminyl repeats (34%) when calculated on the basis of the results of Figure 9 (see Table I). They are also heterogeneous in sialic acid distribution, and monosialosyl (37%), disialosyl (43%), and trisialosyl (20%) saccharides are present when calculated on the basis of the results of Figure 10. The carbohydrate chains at Asn^{38} are composed of triantennary (5%), tetraantennary (49%), and tetraantennary with *N*-acetyllactosaminyl repeats (46%). These carbohydrate

chains are divided into monosialosyl (14%), disialosyl (39%), and trisialosyl (47%) saccharides. The carbohydrate chains attached at Asn^{83}, on the other hand, are relatively homogeneous in the core structures and mainly composed of tetraantennary saccharides (85%), in addition to triantennary (6%) and tetraantennary with one *N*-acetyllactosaminyl repeat (9%). They are sialylated with one (20%), two (45%), or three (35%), as shown in Figure 10.

It is interesting to correlate these findings with the protein structure surrounding the glycosylation sites. Figure 2 illustrates that N-24 and N-38 are relatively close to each other. They also contain similar sets of carbohydrate chains when the asialo forms are regarded. However, they differ significantly in sialylation, and the carbohydrate chains at Asn^{38} are much more sialylated than those at Asn^{24}. On the other hand, the glycans attached at Asn^{83} apparently belong to a domain different from that at Asn^{24} and Asn^{38} (see Figure 2). The carbohydrate chains attached at Asn^{83} are relatively homogeneous in the core structure (Figure 9), but heterogeneously sialylated (Figure 10). These results indicate that the peptide structures surrounding the glycosylation sites are clearly important factors influencing the kind of carbohydrate chains formed.

As described in the introduction, the carbohydrate moiety of erythropoietin is essential for its function in vivo. When sialic acid residues of erythropoietin were removed, the activity of erythropoietin was diminished. The loss of activity can be explained by the rapid clearance from the blood circulation by a galactose binding protein of hepatic cells (Goldwasser et al., 1974). Furthermore, we have recently found that the attachment of poly(*N*-lactosaminyl) side chain enhances the clearance from the blood circulation (Fukuda et al., 1988). These results indicate that the carbohydrate moiety of erythropoietin greatly influences the effective concentration of the protein in vivo. It will be interesting to investigate whether the carbohydrate moiety at a particular site is preferentially bound to a galactose binding lectin in hepatic cells. Another possible role of the carbohydrate is in the binding of erythropoietin to a receptor. It is noteworthy that the binding site of erythropoietin is apparently close to the attachment site of *O*-glycans (Sytowski & Donahue, 1987). It is possible that the attachment of proper *O*-glycans is essential to sustain necessary conformation for the binding of erythropoietin to receptors.

Analysis of variations of glycosylation depending on attachment sites has been reported from several laboratories [for a review, see Kornfeld and Kornfeld (1985)]. In particular, Anderson and Grimes (1982) showed in a mouse myeloma IgM that each glycosylation site has a unique set of heterogeneous saccharides which differ from saccharides at other sites. Similar findings were also reported in porcine ribonuclease (Kabasawa & Hirs, 1972). Parekh et al. (1987) reported on a rat thymocyte thy-1 that *N*-acetyllactosaminyl repeats can be found preferentially in two out of three glycosylation sites. Interestingly, the more complex saccharides can be found in sites close to the carboxyl-terminal region in the thy-1 molecules. In addition, two glycosylation sites, which attach *N*-acetyllactosamine repeats, have a similar degree of sialylation.

It is intriguing that the carbohydrate chains attached at Asn^{24} and Asn^{38} in human erythropoietin differ greatly in the degree of sialylation despite the fact that they both contain fully processed carbohydrates such as tetraantennary saccharides with *N*-acetyllactosamine repeats. It has been shown previously that the extent of oligosaccharide processing correlates with the susceptibility to endo H. When several different glycosylation sites are present in one protein, it was found that endo H preferentially cleaves the oligosaccharides at the sites which are normally processed to complex-type units (Natowicz et al., 1982; Hsieh et al., 1983; Trimble et al., 1983). These findings are consistent with the idea that physical accessibility of the oligosaccharides to processing enzymes can control its maturation (Kornfeld & Kornfeld, 1985). It is tempting to speculate, therefore, that the elongation of the carbohydrate chain at Asn^{24} is possible until the terminal sugars such as galactose reach the neighboring groups so that another glycosyl transferase can no more penetrate to its acceptor structure. Such a limiting environment could be due either to the neighboring polypeptide backbone or to the neighboring carbohydrate chains (in this case, the carbohydrate chain at Asn^{38}) (Sutton & Phillips, 1983). In fact, these two possibilities were suggested in fowl plague virus hemagglutinin glycoprotein (Keil et al., 1985). Further studies to understand the steric structure of erythropoietin are essential to prove this hypothesis.

ACKNOWLEDGMENTS

We thank Dr. Tsutomu Kawaguchi (Chugai Pharmaceuticals Co., Ltd.) for initiating this joint project, Dr. Michael Recny for useful discussion, Dr. Friedrich Piller for critical reading of the manuscript, and Tami Clevenger for secretarial assistance.

Registry No. Erythropoietin, 11096-26-7; *N*-acetyllactosamine, 32181-59-2.

REFERENCES

Al-Khatti, A., Veith, R. W., Papayannopoulou, T., Fritsch, E. F., Goldwasser, E., & Stamatoyannopoulous, G. (1987) *N. Engl. J. Med. 317*, 415–420.

Anderson, D. R., & Grimes, W. J. (1982) *J. Biol. Chem. 257*, 14858–14864.

Baer, A. N., Dessypris, E. N., Goldwasser, E., & Krantz, S. B. (1987) *Br. J. Haematol. 66*, 559–564.

Carr, S. A., & Roberts, G. D. (1986) *Anal. Biochem. 256*, 194–201.

Cavins, J. F., & Friedman, M. (1970) *Anal. Biochem. 35*, 489–493.

Ciucanu, I., & Kerek, F. (1984) *Carbohydr. Res. 131*, 209–217.

Dell, A. (1987) *Adv. Carbohydr. Chem. Biochem. 45*, 19–72.

Eschbach, J. W., Egrie, J. C., Dowwing, M. R., Browne, J. K., & Adamson, J. W. (1987) *N. Engl. J. Med. 316*, 73–78.

Fukuda, M., Carlsson, S. R., Klock, J. C., & Dell, A. (1986) *J. Biol. Chem. 261*, 12796–12806.

Fukuda, M. N., Sasaki, H., Lopez, L., & Fukuda, M. (1988) *Blood* (in press).

Gillece-Castro, B. L., Fisher, S. J., Tarentino, A. L., Peterson, D. L., & Burlingame, A. L. (1987) *Arch. Biochem. Biophys. 256*, 194–201.

Goldwasser, E., & Kung, C. K. H. (1968) *Ann. N.Y. Acad. Sci. 149*, 49–53.

Goldwasser, E., Kung, C. K. H., & Eliason, J. (1974) *J. Biol. Chem. 249*, 4202–4206.

Grant, G. A., Saccettini, J. C., & Wedgus, H. G. (1983) *Biochemistry 22*, 354–358.

Hakomori, S. (1964) *J. Biochem. (Tokyo) 55*, 205–208.

Hsieh, P., Rosner, M. R., & Robbins, P. W. (1983) *J. Biol. Chem. 258*, 2555–2561.

Jacobs, K., Shoemaker, C., Rudersdorf, R., Neill, S. D., Kaufman, R. M., Mufson, A., Sheehra, J., Jones, S. S.,

Hewick, R., Fitch, E. F., Kawakita, M., Shimizu, T., & Miyake, T. (1985) *Nature (London) 313*, 806-810.
Jakel, P. A., Weijer, W. J., & Beintema, J. J. (1983) *Anal. Biochem. 134*, 347-354.
Johnson, R. S., & Biemann, K. (1987) *Biochemistry 26*, 1209-1214.
Kabasawa, I., & Hirs, C. H. W. (1972) *J. Biol. Chem. 247*, 1610-1624.
Keil, W., Geyer, R., Dabrowski, J., Dabrowski, U., Nieman, H., Stirm, S., & Klenk, H. D. (1985) *EMBO J. 4*, 2711-2720.
Kornfeld, R., & Kornfeld, S. (1985) *Annu. Rev. Biochem. 54*, 631-664.
Lai, P.-H., Everett, R., Wang, F.-F., Arakawa, T., & Goldwasser, E. (1986) *J. Biol. Chem. 261*, 3116-3121.
Lin, F. K., Suggs, S., Lin, C. H., Browne, J. K., Smalling, R., Egrie, J. C., Chen, K. D., Fox, G. M., Martin, F., Stabinsky, Z., Badrawi, S. M., Lai, P. M., & Goldwasser, E. (1985) *Proc. Natl. Acad. Sci. U.S.A. 82*, 7580-7584.
Lowy, P. H., Keighley, G., & Borsook, H. (1960) *Nature (London) 185*, 102-103.
Lukowsky, W. A., & Painter, R. H. (1972) *Can. J. Biochem. 50*, 909-917.
McDonald, J. D., Lin, F.-K., & Goldwasser, E. (1986) *Mol. Cell. Biol. 6*, 842-848.
Meek, J. L. (1980) *Proc. Natl. Acad. Sci. U.S.A. 77*, 1632-1636.
Miyake, T., Kung, C. K. H., & Goldwasser, E. (1977) *J. Biol. Chem. 252*, 5558-5564.
Natowicz, M., Baenziger, J. V., & Sly, W. S. (1982) *J. Biol. Chem. 257*, 4412-4420.
Parekh, R. B., Tse, A. G. D., Dwek, R. A., William, A. F., & Rademacher, T. W. (1987) *EMBO J. 6*, 1233-1244.
Plummer, T. H., Jr., Elder, J. H., Alexander, S., Phelan, A. W., & Tarentino, A. L. (1984) *J. Biol. Chem. 259*, 10700-10704.
Powell, J. S., Berkner, K. L., Lebo, R. V., & Adamson, J. W. (1986) *Proc. Natl. Acad. Sci. U.S.A. 83*, 6465-6469.
Rambach, W. A., Shaw, R. A., Cooper, J. A. D., & Apt, H. L. (1958) *Proc. Soc. Exp. Biol. Med. 99*, 482-483.
Recny, M. A., Scoble, H. A., & Kim, Y. (1987) *J. Biol. Chem. 262*, 17156-17163.
Robb, R. J., Kutny, R. M., Panico, M., Morris, H. R., & Chowdry, V. (1984) *Proc. Natl. Acad. Sci. U.S.A. 81*, 6486-6490.
Sasaki, H., Bothner, B., Dell, A., & Fukuda, M. (1987) *J. Biol. Chem. 262*, 12059-12076.
Sutton, B. J., & Phillips, D. C. (1983) *Biochem. Soc. Trans. 11*, 130-132.
Sytkowski, A. J., & Donahue, K. A. (1987) *J. Biol. Chem. 262*, 1161-1165.
Townsend, R. R., Heller, D. N., Fenselan, C. C., & Lee, Y. C. (1984) *Biochemistry 23*, 6389-6392.
Trimble, R. B., Maley, F., & Chu, F. K. (1983) *J. Biol. Chem. 258*, 2555-2567.
Winearls, C. G., Oliver, D. O., Pippard, M. J., Reid, C., Downing, M. R., & Cotes, P. M. (1986) *Lancet ii*, 1175-1178.

Binding of Ca^{2+} to the Calcium Adenosinetriphosphatase of Sarcoplasmic Reticulum†

Joanne R. Petithory and William P. Jencks*
Graduate Department of Biochemistry, Brandeis University, Waltham, Massachusetts 02254
Received March 30, 1988; Revised Manuscript Received July 5, 1988

ABSTRACT: The binding of Ca^{2+} and the resulting change in catalytic specificity that allows phosphorylation of the calcium ATPase of sarcoplasmic reticulum by ATP were examined by measuring the amount of phosphoenzyme formation from [^{32}P]ATP, or ^{45}Ca incorporation into vesicles, after the simultaneous addition of ATP and EGTA at different times after mixing enzyme and Ca^{2+} (25 °C, pH 7.0, 5 mM $MgSO_4$, 0.1 M KCl). A "burst" of calcium binding in the presence of high [Ca^{2+}] gives ~12% phosphorylation and internalization of two Ca^{2+} at very short times after the addition of Ca^{2+} with this assay. This shows that calcium binding sites are available on the cytoplasmic-facing side of the free enzyme. Calcium binding to these sites induces the formation of $^{c}E{\cdot}Ca_2$, the stable high-affinity form of the enyzme, with $k = 40\ s^{-1}$ at saturating [Ca^{2+}] and a half-maximal rate at approximately 20 μM Ca^{2+} (from $K_{diss} = 7.4 \times 10^{-7}$ M for Ca·EGTA). The formation of $^{c}E{\cdot}Ca_2$ through a "high-affinity" pathway can be described by the scheme $E \overset{1}{\rightleftharpoons} {}^{c}E{\cdot}Ca_1 \overset{2}{\rightleftharpoons} {}^{c}E{\cdot}Ca_2$, with $k_1 = 3 \times 10^6\ M^{-1}\ s^{-1}$, $k_2 = 4.3 \times 10^7\ M^{-1}\ s^{-1}$, $k_{-1} = 30\ s^{-1}$, $k_{-2} = 60\ s^{-1}$, $K_1 = 9 \times 10^{-6}$ M, and $K_2 = 1.4 \times 10^{-6}$ M. The approach to equilibrium from E and 3.2 μM Ca^{2+} follows $k_{obsd} = k_f + k_r = 18\ s^{-1}$ and gives $k_f = k_r = 9\ s^{-1}$. The rate of exchange of ^{45}Ca into the inner position of $^{c}E{\cdot}Ca_2$ shows an induction period and is not faster than the approach to equilibrium starting with E and ^{45}Ca. The dissociation of ^{45}Ca from the inner position of $^{c}E{\cdot}{}^{45}Ca{\cdot}Ca$ in the presence of 3.2 μM Ca^{2+} occurs with a rate constant of 7 s^{-1}. These results are inconsistent with a slow conformational change of free E to give ^{c}E, followed by rapid binding–dissociation of Ca^{2+}.

The binding of two calcium ions to cytoplasmic-facing sites on the calcium ATPase of SRV[1] is of interest because it is a critical vectorial step in the transport process and it initiates the change in catalytic specificity of the enzyme that allows

† Publication No. 1669 from the Graduate Department of Biochemistry, Brandeis University. This research was supported in part by grants from the National Institutes of Health (GM20888) and the National Science Foundation (PCM-8117816).

[1] Abbreviations: SRV, sarcoplasmic reticulum vesicles; EGTA, ethylene glycol bis(β-aminoethyl ether)-*N,N,N',N'*-tetraacetic acid; MOPS, 4-morpholinepropanesulfonic acid; P_i, inorganic phosphate.

0006-2960/88/0427-8626$01.50/0